ACS Sustainable Chemistry & Engineering

Research Article

pubs.acs.org/journal/ascecg

Assembly of Layered Silicate Loaded Quaternized Chitosan/Reduced Graphene Oxide Composites as Efficient Absorbents for Double-Stranded DNA

Xiaoyun Li,[†] Yang Han,[†] Yunzhi Ling,[†] Xiaoying Wang,*[,†] and Runcang Sun[†,‡]

[†]State Key Laboratory of Pulp and Paper Engineering, South China University of Technology, 381 Wushan Road, Tianhe District, Guangzhou 510640, People's Republic of China

[‡]Institute of Biomass Chemistry and Technology, Beijing Forestry University, No. 35 Tsinghua East Road, Haidian District, Beijing 100083, People's Republic of China

ABSTRACT: In this study, we prepared stable reduced graphene oxide (rGO) solutions with renewable resource quaternized chitosan (QCS) and layered silicate as green reducing and stabilizing agents. Rectorite (REC) and organic rectorite (OREC) are typical layered silicate employed in this work. UV−visible absorption spectroscopy, Fourier transform infrared spectroscopy, X-ray photoelectron spectroscopy, and Raman spectroscopy results showed the good reducing effect of QCS to produce rGO. Transmission electron microscopy, atomic force microscope, and X-ray diffraction results showed that rGO nanosheets were loaded with layered silicate through cation exchange to get a rGO/QCS/layered silicate composite. The high zeta potential (+41.4 mV) of the rGO/QCS composite showed the good stabilizing effect of QCS, and the higher zeta potential of rGO/QCS/OREC (+38.5 mV) than that of rGO/QCS/REC (+37.3 mV) indicated that OREC had a better stabilizing effect than REC. The possible assembly mechanism of the rGO/QCS/layered silicate composite was electrostatic interaction and cation exchange. The addition of the layered silicate improved the thermal stability of the composite, and rGO/QCS/OREC showed high uptake (425 μg/mg) toward double-stranded DNA (dsDNA).

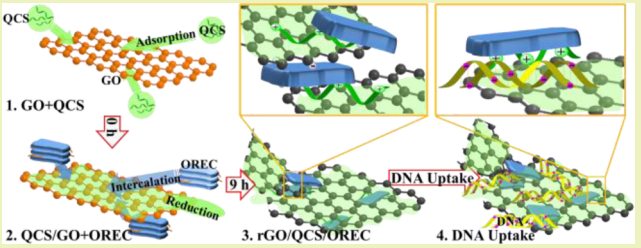

KEYWORDS: *Reduced graphene oxide (rGO), Quaternized chitosan (QCS), Layered silicate, Green reducing, Stabilizing, DNA Uptake, Thermal stability*

INTRODUCTION

Graphene and its composites have drawn much interest in recent years due to the numerous potential applications in catalysis, high-strength conductive composite films, electronics, energy conversion and storage, biotechnology, sensing, and so on,[1,2] while the preparation method of graphene and its composites is vitally important to the applications of graphene. Among the existing graphene preparation methods, chemical reduction of graphene oxide (GO) is the mostly used method,[1] but there are still two problems inherent in this method: toxic reducing agents[3−5] and instability of reduced graphene oxide (rGO) sheets.[6,7] Therefore, preparing graphene and its composites with green reducing and strong stabilizing agents deserves more attention.

Chitosan, obtained from crustacean shells, insects, molluscan organs, and fungi, is one of the most abundantly occurring biopolymers and can be used in antibacterial filtration, drug release, tissue engineering, and biosensors.[8−11] Chitosan and its derivatives are well known as green reducing and stabilizing agents for nanomaterials.[3] Quaternized chitosan (QCS) is a water-soluble chitosan derivative synthesized by grafting quaternary ammonium groups onto chitosan chains, which can act as a reducing and stabilizing agent due to the many hydroxyl groups (−OH) and quaternary ammonium groups on its chains. Our previous work has indicated that QCS could work as an efficient reducing and stabilizing agent in the synthesis of silver and gold nanoparticles.[12,13] But the reducing and stabilizing effects of QCS on GO have not been reported. What is more, the grafting of positively charged quaternary ammonium groups enabled chitosan to interact with negatively charged substances in all pH values.

In addition, it is noted that engineering the graphene surfaces through either covalent or noncovalent approaches has been proved to be feasible methods to obtain well dispersed rGO in aqueous solution. Noncovalent modifications avoid tedious chemical reactions compared with covalent grafting approaches.[14] Liu et al. stabilized rGO in the presence of montmorillonite through noncovalent strategy.[7] Layered silicates, natural minerals with large surface area and chemical and mechanical stability,[15] are known to be potentially useful as supports for dispersed semiconductor particles, metals, and metal oxides.[16] Rectorite (REC) is a similar mineral resource

Received: May 12, 2015
Revised: June 23, 2015
Published: June 25, 2015

DOI: 10.1021/acssuschemeng.5b00404
ACS Sustainable Chem. Eng. 2015, 3, 1846−1852

layered structure with montmorillonite, which can also display a stabilizing effect.[17,18] It is noted that its interlayer distance is larger than that of montmorillonite, and after modifying by surfactants, the obtained organic rectorite (OREC) has a larger interlayer distance than REC.[19,20] However, until now, there is no report on stabilizing rGO with REC or OREC.

In this paper, we first tried to combine the reducing and stabilizing effect of QCS and layered silicate in the preparation of rGO. QCS performed a green reducing effect on GO, and layered silicate (OREC and REC) was loaded onto rGO through cation exchange. Water-stable rGO/QCS/REC and rGO/QCS/OREC composites were obtained. The possible mechanism is discussed briefly. Finally, the prepared composites were used to adsorb double-stranded DNA (dsDNA).

MATERIALS AND METHODS

Materials. Natural graphite flakes were provided by XFNANO Materials Tech Co., Ltd. (Nanjing, China). Chitosan was supplied by Jinan Haidebei Marine Bioengineering Co., Ltd. (Shandong, China). Calcium rectorite (REC) refined from the clay minerals was provided by Hubei Mingliu Inc., Co. (Hubei, China). Gemini surfactant (18-3-18, $C_{43}H_{92}N_2Cl_2$, FW: 707) was purchased from Henan Titaning Chemical Technology Co., Ltd. (Henan, China). Other reagents and solvents were analytical grade. All materials were used without further purification. The gene of *Penicillium camembertii* Lipase (Genbank ID: D90315.1) cloned in plasmid pGAPZaA was used as the template. Primers used for DNA amplification were designed using QuickChange Primer Design (http://www.genomics.agilent.com/primerDesignProgram.jsp) and synthesized by Life Technologies. Primer sequences were as follows:

Avr II forward: 5′-CCTAGGAAATTTTACTCTGCTGGAGAGCTT-3′

Avr II reverse: 5′-GACGGTAACGGGCGGTGGAAGGAGAGAGAA-3′

Polymerase chain reaction (PCR) was performed in a final volume of 50 μL containing template DNA, primers, 62.5 U of PrimeSTAR HS DNA Polymerase (Takara), and water. The amplification program was as follows: 3 min at 98 °C, followed by 30 cycles of 10 s at 98 °C, 15 s at 60 °C, 3 min and 50 s at 72 °C, and then 7 min at 72 °C.

Preparation of QCS and OREC. QCS was prepared according to previous work.[12] Briefly, chitosan was quaternized with 2,3-epoxypropyltrimethylammonium chloride in microwave irradiation at 800 W and 75 °C for 70 min. After reaction, QCS was filtered and washed with acetone. QCS was obtained after dialysis and lyophilization. The degree of substitution of quaternization groups was 0.87 ± 0.03.

OREC was synthesized according to a previous study;[18] REC was reacted with organic surfactant Gemini 18-3-18 in microwave irradiation at 800 W and 80 °C. After reacting for 1 h, the reaction solution was washed with 50% isopropanol. OREC was obtained after lyophilization.

Synthesis of Graphite Oxide. Graphite oxide was prepared according to the modified Hummers method.[21] One gram of graphite powder was added to 23 mL of cold concentrated H_2SO_4. The mixture was stirred for 30 min, and 3 g of $KMnO_4$ was added and then reacted for 30 min at temperature lower than 20 °C. The mixture was maintained at 35 °C for 2 h. Afterward, 46 mL of distilled water was gradually added into the mixture, and the temperature was kept at 98 °C for 30 min. The reaction was terminated with 140 mL of distilled water followed by 5 mL of 30% H_2O_2. For purification, the mixture was washed with 10% HCl and distilled water several times. The graphite oxide was obtained by lyophilization.

Preparation of rGO/QCS/Layered Silicate Composites. A total of 0.1 g of layered silicate (REC or OREC) and 0.01 g of GO were dispersed in water separately, and the pH of GO solution was adjusted to 9 with NaOH solution. 5 mL of QCS (0.5 wt %) solution was gradually added into GO with stirring, and the temperature was set at 90 °C for 30 min. Afterward, 2.5 mL of QCS (3 wt %) solution was gradually added into the mixture, after which layered silicate dispersion was added. The UV−vis absorbance value was measured to monitor the reaction. Finally, rGO/QCS/layered silicate was obtained after reacting for 9 h. The sample of rGO/QCS was prepared without layered silicate. To better study the structure and morphology rGOs, the samples for X-ray photoelectron spectroscopy (XPS), Raman, atomic force microscope (AFM), and transmission electron microscopy (TEM) were centrifuged at 15,000 rpm to wash free QCS. The samples are listed in Table 1.

Table 1. Samples with Free QCS and without Free QCS

samples	with free QCS	without free QCS
without layered silicate	rGO/QCS	rGO
with REC	rGO/QCS/REC	rGO/REC
with OREC	rGO/QCS/OREC	rGO/OREC

Characterizations. UV−visible absorption spectroscopy (UV−vis) was obtained by TU-1810 (PGeneral, China). Each sample was scanned from 500 to 200 nm. Fourier transform infrared spectroscopy (FT-IR) was measured by a Tensor 27 (Bruker, Germany) under dry air at room temperature by a KBr pellet method. Each sample was scanned from 4000 to 400 cm^{-1} with a resolution of 4 cm^{-1}. XPS measurements were recorded on a Thermo Fisher Scientific ESCALAB 250 using monochromatrized Al Kα excitation. All binding energies were calibrated by using the contaminant carbon (C 1s = 284.8 eV) as a reference. The Raman spectra were obtained on a Horiba Jobin Yvon LabRAM Aramis automatic laser Raman spectrometer using a 633 nm line of Ar^+ ion laser as the excitation source at room temperature.

AFM images were obtained with Dimension Fastscan Bio (Bruker, Germany). The diluted samples were immediately deposited onto freshly cleaved mica surfaces and dried at room temperature. JEM-2010HR transmission electron microscopy (JEOL, Japan) was used to investigate the microstructure of the composites at an accelerating voltage of 200 kV. X-ray diffraction (XRD) of powder samples was measured by a D8 advance X-ray diffractometer (Bruker, Germany) with a Cu target and Kα radiation (λ = 0.15418 nm) at 40 kV and 50 mA at 20 °C. Measurements of zeta potentials were performed three times with a Zetasizer Nano-ZS at 100 V (Malvern, U.K.). The concentration of samples was 0.1%. Thermogravimetric analysis (TGA) was carried out on a TGA Q500 (TA, U.S.A.). Samples were heated from room temperature to 700 °C at a heating rate of 10 °C/min in high-purity flowing nitrogen atmosphere (25 mL/min).

Adsorption of DNA. Adsorption studies toward dsDNA were done in PBS. Stock solution of dsDNA was prepared by dissolving in PBS solution, and then rGO, QCS, rGO/QCS, rGO/QCS/REC, and rGO/QCS/OREC were suspended in the stock solution. After aging for 24 h, they were centrifuged at 15,000 rpm, and the supernatant liquid was tested in Nanovue Plus to quantify the remaining dsDNA concentration.

$$\text{DNA Uptake} = \frac{(C_0 - C_t) \times V_{DNA}}{C \times V_{adsorbent}}$$

where C_0 and C_t are the initial and actual concentrations of DNA tested with Nanovue Plus, respectively, C is the concentration of adsorbents, and V_{DNA} and $V_{adsorbent}$ are volumes of DNA and adsorbent, respectively.

RESULTS AND DISCUSSION

Reduction of GO with QCS. The UV−vis absorption spectra of GO and rGOs are shown in Figure 1; two peaks centered at 230 and 300 nm in GO correspond to the $\pi-\pi^*$ transition of aromatic C═C bonds and the n-π^* transition of the C═O bond, respectively.[7] As the reaction proceeded, the peak at 300 nm disappeared, and the peak at 230 nm gradually

DOI: 10.1021/acssuschemeng.5b00404
ACS Sustainable Chem. Eng. 2015, 3, 1846−1852

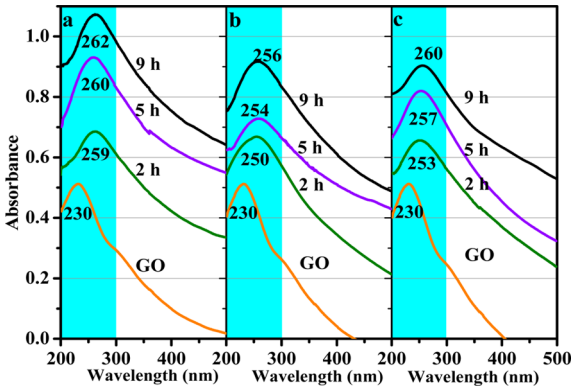

Figure 1. UV−vis absorption spectra of rGOs in QCS solution at different times: (a) without layered silicate, (b) with REC, and (c) with OREC.

red-shifted to 262 nm after reacting for 9 h. The absorbance increased significantly, indicating that the electronic conjugation within the graphene sheets was restored gradually with QCS as the reducing agent.[3]

From Figure 1b and c, we can see that the peak at 230 nm red-shifted to 256 and 260 nm with layered silicate in the system, indicating the extent of reduction was a little lower than that without layered silicate.[22] This can be explained that part of the QCS might react with layered silicate, and thus the reduction was weakened.

Figure 2 shows the FT-IR spectra of the samples. In the spectrum of GO, the broad absorption band at 3408 cm^{-1} was

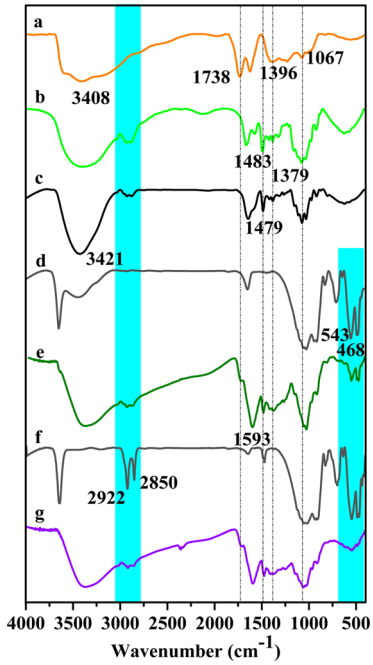

Figure 2. FT-IR spectra of (a) GO, (b) QCS, (c) rGO/QCS, (d) REC, (e) rGO/QCS/REC, (f) OREC, and (g) rGO/QCS/OREC composites.

assigned to the OH groups of GO.[7] The peak at 1738 cm^{-1} was from carbonyl and carboxylic groups. The peak at 1067 cm^{-1} was from carbonyl, carboxylic, and epoxy groups. The latter two peaks indicate that GO was prepared successfully.[23] Compared to GO, the peak at 1738 cm^{-1} disappeared in rGO/QCS, indicating the successful reduction process and good reducing effect of QCS. The peak at 1738 cm^{-1} still occurs weakly in rGO/QCS/REC and rGO/QCS/OREC, indicating the reduction effect of QCS was a bit weakened with layered silicate in the system. These results correspond with UV−vis results. In the spectrum of rGO/QCS, the peak at 1483 cm^{-1} belonging to the twist motion of $-CH_2-$ in quaternary groups of QCS was greatly reduced and shifted to lower frequency. This result indicates that the quaternary group of QCS had a reducing effect, which is in accordance with our previous work.[12] In the spectra of rGO/QCS/REC and rGO/QCS/OREC, the peaks at 543 and 468 cm^{-1} belonged to layered silicate, indicating the existence of layered silicate in the product.

In the FT-IR spectra of rGO/QCS/OREC, the peaks at 2922 and 2850 cm^{-1} belonging to the Gemini surfactant were greatly reduced when compared to rGO/QCS/REC, indicating a decrease in surfactants in the interlayer region, which indirectly suggests rGO nanosheets replaced the surfactants in the interlayer region of OREC.[23]

The reduction of GO was also investigated by XPS. Figure 3 shows the XPS spectra of GO and rGOs. Compared to GO, a

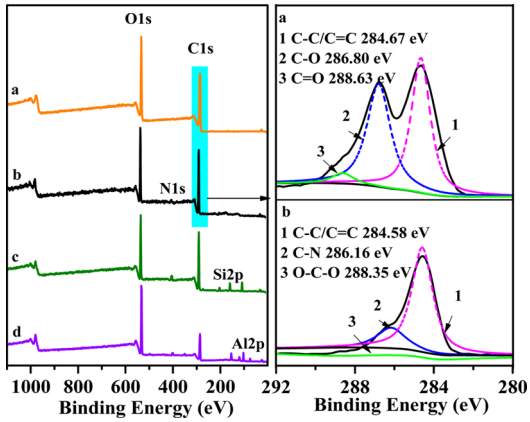

Figure 3. XPS spectra of (a) GO, (b) rGO, (c) rGO/REC, and (d) rGO/OREC composites.

new peak corresponding to N 1s (402.81 eV) in rGOs was observed, indicating some QCS was tightly absorbed onto rGOs nanosheets,[3] though free QCS was washed away. The C 1s XPS spectrum of GO clearly indicates a considerable degree of oxidation, with three different components corresponding to carbon atoms in different functional groups: nonoxygenated ring C (C−C), C in C−O bonds (C−O), and carboxylate carbon (O−C═O). The areas of the three C 1s components showed that the nonoxygenated ring C (C−C) is about 49.4% for GO, while 87.1% for rGO (Figure 3). These results reveal that most of the oxygen functional groups in GO were removed,[24] and this is in accordance with UV−vis and FT-IR results.

Raman spectroscopy is a widely used tool to characterize the structure of graphene-based materials. As shown in Figure 4, we can see the G band at 1595 cm^{-1} and the D band at 1321 cm^{-1}.[25] The G band and D band correspond to sp^2 hybridized disordered carbon and sp^3 hybridized carbon, respectively. Changes in the relative intensities of the D band to G band (I_D/I_G) indicate the changes in the electronic conjugation state of the GO during reduction. The Raman spectra of rGOs showed higher I_D/I_G ratios (0.92, 1.13, and 1.09 for rGO, rGO/REC, and rGO/OREC, respectively) than that of GO (0.65),

DOI: 10.1021/acssuschemeng.5b00404
ACS Sustainable Chem. Eng. 2015, 3, 1846−1852

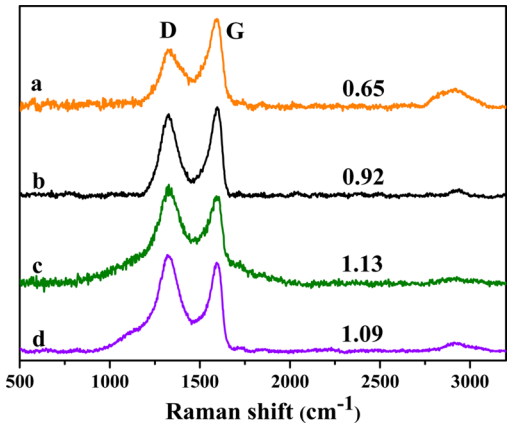

Figure 4. Raman spectra of (a) GO, (b) rGO, (c) rGO/REC, and (d) rGO/OREC composites.

implying a decreased size of the sp^2 domains upon the reduction of GO,[7,26] which further demonstrates the effective reduction of GO by QCS, and this is in accordance with previous works.[3,24]

Loading of Layered Silicate over rGO Nanosheets. Figure 5 shows the AFM images and height profiles of GO and rGOs. The heights of the exfoliated nanosheets in GO and rGO were 1.9 and 1.5 nm, respectively. The decrease in thickness could be explained by the removal of oxygen functional groups during the reduction process.[4] With the addition of layered silicate into the system, the height of the nanosheets was greatly increased to 13.5 nm, and this increment in thickness was due to the layered silicate loading over rGO nanosheets. There was a 12 nm increment in both rGO/REC and rGO/OREC compared with that of rGO, indicating that the loading amounts of REC and OREC on rGO were similar.[27]

The TEM image of rGO (Figure 6a) displayed the sheet structure of rGO, and the TEM image of OREC (Figure 6b) extensively displayed the typical layered structure of the layered silicate.[28] In the TEM image of rGO/OREC, the dark entities were the cross section of OREC[29,30] and the gray areas were rGO matrix. EDS analysis taken from the indicated region reveals the existence of Al and Si, confirming that OREC were loaded over rGO nanosheets. Compared to OREC, the interlayer of rGO/OREC was enlarged clearly, indicating that

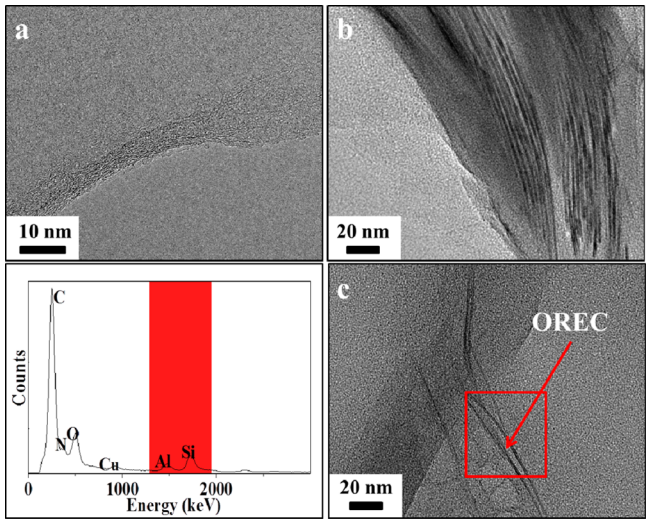

Figure 6. TEM images of (a) rGO, (b) OREC, and (c) rGO/OREC composites and the corresponding EDS results.

rGO nanosheets entered into the clay layer space. Those are in accordance with AFM results.

The XRD patterns of the samples are shown in Figure 7. Graphite had a strong diffraction peak at about 26.5° (002),

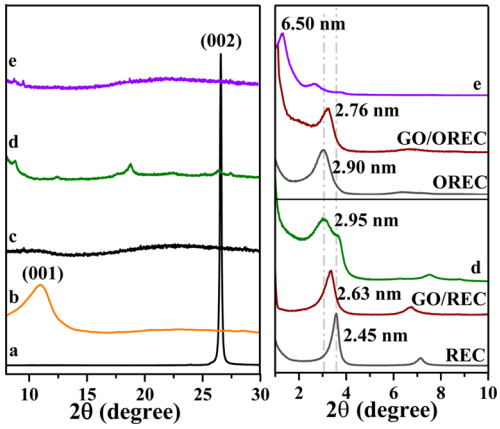

Figure 7. XRD patterns of (a) graphite, (b) GO, (c) rGO/QCS, (d) rGO/QCS/REC, and (e) rGO/QCS/OREC composites.

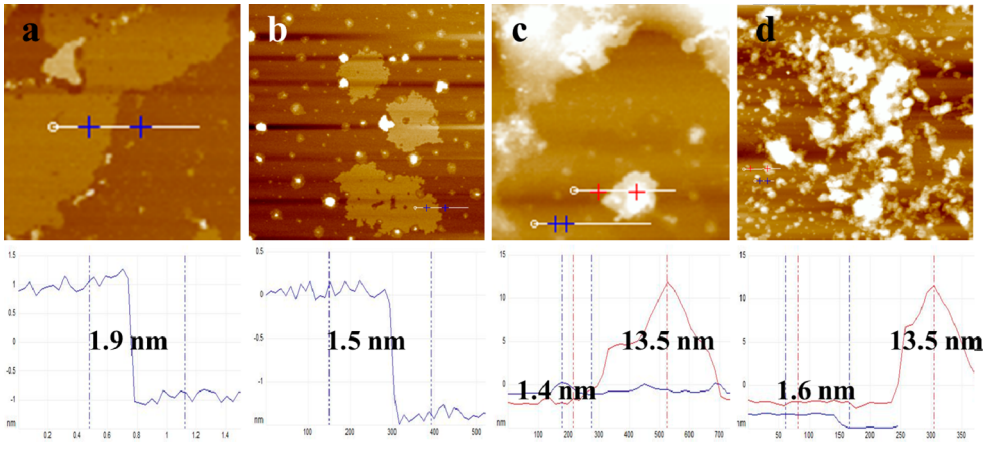

Figure 5. AFM images (3 μm × 3 μm) of (a) GO, (b) rGO, (c) rGO/REC, and (d) rGO/OREC composites.

DOI: 10.1021/acssuschemeng.5b00404
ACS Sustainable Chem. Eng. 2015, 3, 1846−1852

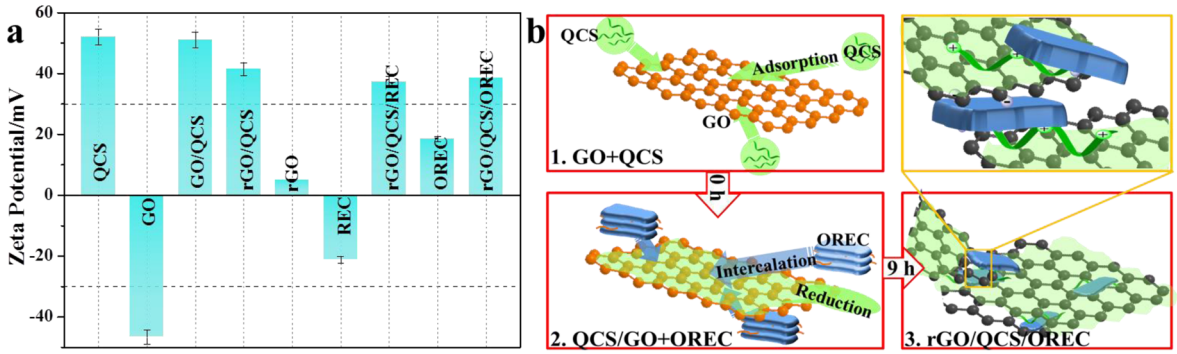

Figure 8. Zeta potential of prepared samples (a) and possible mechanism for the preparation of rGO/QCS/OREC composite (b).

which represents an interlayer distance of 0.34 nm (Figure 7a), but this peak disappeared in GO. A new diffraction peak for GO at 11.0° (001) with an interlayer distance of 0.81 nm was observed (Figure 7b), indicating a complete oxidation of graphite into graphite oxide.[24] In the spectra of rGO/QCS, rGO/QCS/REC, and rGO/QCS/OREC, no characteristic peak of graphite was observed, which indicated the restacking of graphene nanosheets was effectively prevented, just as the previous work.[31] In addition, the disappearance of the peak at 11.0° also indicated the reduction of GO.[3]

To better know the interaction between GO and layered silicate, the control samples labeled as GO/REC and GO/OREC were prepared without QCS, and the XRD results are shown in Figure 7. The interlayer distance of OREC was 2.90 nm, which is larger than 2.45 nm of REC, which indicated that the Gemini surfactant had been intercalated into interlayers of REC. It is clear that compared to the d_{001} distance of REC (2.45 nm) and OREC (2.90 nm), the d_{001} distance of GO/REC (2.63 nm) and GO/OREC (2.76 nm) showed no obvious difference with the corresponding layered silicate. In contrast, the d_{001} distance of rGO/QCS/REC (2.95 nm) and rGO/QCS/OREC (6.50 nm) enlarged greatly, indicating the rGO nanosheets were intercalated into clay layer space.

Possible Mechanism for Preparation of rGO/QCS/Layered Silicate Composites. The above reduction and loading results combining with the zeta potential in Figure 8a verify our supposition in Figure 8b. QCS (+52.1 mV) was absorbed onto GO (−46.7 mV) nanosheets through electrostatic interaction,[32] just as cationic chitosan adhered to negatively charged surfaces of multiwalled carbon nanotubes.[33] Then OREC and REC were loaded over GO/QCS composite (+51.1 mV) through cation exchange, just as graphite oxide sheets were intercalated between the layers of anionic clay.[23] During this process, GO (−46.7 mV) was gradually reduced to rGO (+4.98 mV) with QCS, and with the loading of OREC, we got the rGO/QCS/OREC composite. The decrease in zeta potential from +51.1 mV of GO/QCS to +41.4 mV of rGO/QCS can be explained that some positively charged quaternary groups of QCS displayed a reducing effect in the reduction of GO, and the remaining groups performed a stabilizing effect for rGO. This corresponds to FT-IR results. Generally, the dispersion stability can be explained from the zeta potential. High zeta potential indicates stronger positive or negative charges repulsion. So the high zeta potential of rGO/QCS (+41.4 mV) indicates the a good stabilizing effect of QCS. The rGO/QCS/OREC solution (+38.5 mV) was more stable than the rGO/QCS/REC solution (+37.3 mV), which indicates OREC exhibited a stronger stabilizing effect than REC.

Thermal Analysis. The thermal behaviors of the samples are shown in Figure 9. Graphite exhibits almost no mass loss

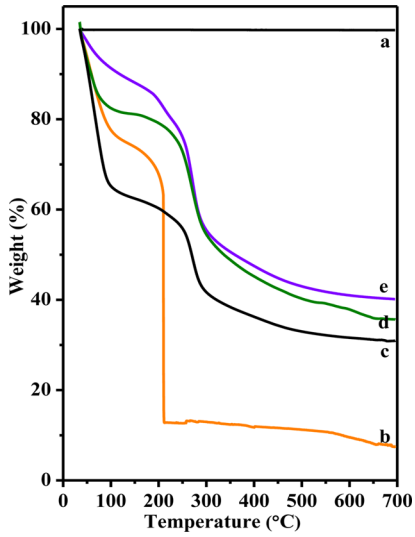

Figure 9. TGA curves of (a) graphite, (b) GO, (c) rGO/QCS, (d) rGO/QCS/REC, and (e) rGO/QCS/OREC composites.

over the temperature range. GO exhibits two steps of significant mass drops at 210 and 637 °C, which are attributed to the removal of oxygen-functional groups and the combustion of the carbon skeleton of GO, respectively.[3] Before 210 °C, rGO/QCS exhibited a larger mass loss than GO, which can be explained by the decomposition of QCS absorbed on the rGO sheets. At 700 °C, rGO/QCS exhibited higher thermal stability than GO because of the removal of oxygen-functional groups with the reduction by QCS. The weight remaining of rGO/QCS (30%) was enhanced to 35% (rGO/QCS/REC) and 40% (rGO/QCS/OREC) due to the excellent thermal stability of layered silicate.

DNA Uptake. Adsorption of biomolecules (DNA, RNA, and proteins) on inorganic materials is highly beneficial and shows applications in gene delivery. The adsorption toward dsDNA after aging for 24 h is shown in Figure 10. All the samples showed strong adsorption capacity toward dsDNA. As expected, rGO showed high DNA uptake because of the large specific surface area.[29] In addition, the strong electrostatic interaction between positively charged QCS (+52.1 mV) and negatively charged DNA made QCS showed a very high DNA uptake (600 μg/mg).[34,35] So rGO/QCS (+41.4 mV) without washing free QCS showed higher DNA uptake (550 μg/mg)

DOI: 10.1021/acssuschemeng.5b00404
ACS Sustainable Chem. Eng. 2015, 3, 1846−1852

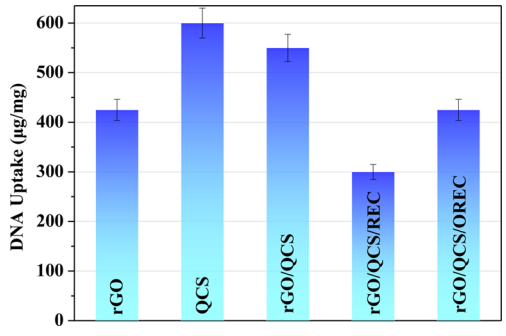

Figure 10. DNA uptake of different samples after 24 h.

than that of rGO, while the decreased DNA uptake of rGO/QCS compared to QCS can be explained with the lower content of QCS. In addition, the DNA uptake of rGO/QCS/OREC and rGO/QCS/REC were 425 and 300 μg/mg, respectively. The higher DNA uptake of rGO/QCS/OREC than that of rGO/QCS/REC was related to the higher zeta potential of rGO/QCS/OREC (+38.5 mV).[29] The samples with layered silicate showed poor DNA uptake than that without layered silicate, which might be explained by two points: lower zeta potential of the samples with layered silicate and loading of layered silicate to reduce the amount of rGO and QCS. Nevertheless, the water-stable rGO/QCS/layered silicate still showed higher DNA uptake compared with previous work,[29] so it has the potential to be a nonviral vector.

CONCLUSIONS

A green approach to synthesize stable rGO solution using QCS and layered silicate as the reducing agent and stabilizing agent has been developed. The layers of GO were electrostatically wrapped with QCS, and then QCS wrapped GO was loaded with layered silicate through cation exchange. During the process, GO was reduced by QCS, and finally, we got rGO/QCS/layered silicate composites. This is a new method to obtain composites based on negatively charged nanosheets and layered silicate through cation exchange, and the cationic polymers works as the glue in this kind of structure. The addition of layered silicate improved thermal stability of rGO. The rGO/QCS/layered silicate composites showed strong adsorption ability toward dsDNA, indicating that the composites might be used as gene delivery. In addition, this work provides a high-value utilization of natural products.

AUTHOR INFORMATION

Corresponding Author

*E-mail: xyw@scut.edu.cn. Tel: +86 20 87111861.

Notes

The authors declare no competing financial interest.

ACKNOWLEDGMENTS

This work was financially supported by the National Natural Science Foundation of China (51403069), Program for New Century Excellent Talents in University (NCET-13-0216), Science & Technology Project of Guangzhou City in China (2012J2200018), and the Fundamental Research Funds for the Central Universities, SCUT (2014ZG0011).

REFERENCES

(1) Bai, H.; Li, C.; Shi, G. Q. Functional composite materials based on chemically converted graphene. *Adv. Mater.* **2011**, *23* (9), 1089−1115.
(2) Wassei, J. K.; Kaner, R. B. Oh, the Places You'll Go with Graphene. *Acc. Chem. Res.* **2013**, *46* (10), 2244−2253.
(3) Guo, Y. Q.; Sun, X. Y.; Liu, Y.; Wang, W.; Qiu, H. X.; Gao, J. P. One pot preparation of reduced graphene oxide (RGO) or Au (Ag) nanoparticle-RGO hybrids using chitosan as a reducing and stabilizing agent and their use in methanol electrooxidation. *Carbon* **2012**, *50* (7), 2513−2523.
(4) Zhou, Y.; Bao, Q. L.; Tang, L. A. L.; Zhong, Y. L.; Loh, K. P. Hydrothermal Dehydration for the "Green" Reduction of Exfoliated Graphene Oxide to Graphene and Demonstration of Tunable Optical Limiting Properties. *Chem. Mater.* **2009**, *21* (13), 2950−2956.
(5) Fan, X. B.; Peng, W. C.; Li, Y.; Li, X. Y.; Wang, S. L.; Zhang, G. L.; Zhang, F. B. Deoxygenation of Exfoliated Graphite Oxide under Alkaline Conditions: A Green Route to Graphene Preparation. *Adv. Mater.* **2008**, *20* (23), 4490−4493.
(6) Alhassan, S. M.; Qutubuddin, S.; Schiraldi, D. A. Graphene arrested in laponite-water colloidal glass. *Langmuir* **2012**, *28* (8), 4009−4015.
(7) Zhang, C.; Tjiu, W. W.; Fan, W.; Yang, Z.; Huang, S.; Liu, T. X. Aqueous stabilization of graphene sheets using exfoliated montmorillonite nanoplatelets for multifunctional free-standing hybrid films via vacuum-assisted self-assembly. *J. Mater. Chem.* **2011**, *21* (44), 18011−18017.
(8) Wang, Q.; Du, Y. M.; Fan, L. H.; Liu, H.; Wang, X. H. Structures and Properties of Chitosan-Starch-Sodium Benzoate Blend Films. *J. Wuhan Uni.* **2003**, *49*, 725.
(9) Hu, X. W.; Tang, Y. F.; Wang, Q.; Li, Y.; Yang, J. H.; Du, Y. M.; Kennedy, J. F. Rheological Behaviors of Chitin in NaOH/Urea Aqueous Solution. *Carbohydr. Polym.* **2011**, *83* (3), 1128−1133.
(10) Ding, F. Y.; Deng, H. B.; Du, Y. M.; Shi, X. W.; Wang, Q. Emerging Chitin and Chitosan Nanofibrous Materials for Biomedical Applications. *Nanoscale* **2014**, *6* (16), 9477−9493.
(11) Yang, Y.; Wang, S. P.; Wang, Y. T.; Wang, X. H.; Wang, Q.; Chen, M. W. Advances in Self-assembled Chitosan Nanomaterials for Drug Delivery. *Biotechnol. Adv.* **2014**, *32* (7), 1301−1316.
(12) Liu, B.; Li, X. Y.; Zheng, C. F.; Wang, X. Y.; Sun, R. C. Facile and green synthesis of silver nanoparticles in quaternized carboxymethyl chitosan solution. *Nanotechnology* **2013**, *24* (23), 235601.
(13) Ling, Y. Z.; Luo, Y. Q.; Luo, J. W.; Wang, X. Y.; Sun, R. C. Synthesis Optimization of Quaternized Chitosan and its Action as Reducing and Stabilizing Agent for Gold Nanoparticles. *J. Macromol. Sci., Part A: Pure Appl.Chem.* **2013**, *50* (12), 1194−1200.
(14) Georgakilas, V.; Otyepka, M.; Bourlinos, A. B.; Chandra, V.; Kim, N.; Kemp, K. C.; Hobza, P.; Zboril, R.; Kim, K. S. Functionalization of Graphene: Covalent and Non-Covalent Approaches, Derivatives and Applications. *Chem. Rev.* **2012**, *112* (11), 6156−6214.
(15) Lu, Y.; Li, X. Y.; Zhou, X. D.; Wang, Q.; Shi, X. W.; Du, Y. M.; Deng, H. B.; Jiang, L. B. Characterization and cytotoxicity study of nanofibrous mats incorporating rectorite and carbon nanotubes. *RSC Adv.* **2014**, *4* (63), 33355−33361.
(16) Prashanth, S. N.; Teradal, N. L.; Seetharamappa, J.; Satpati, A. K.; Reddy, A. V. R. Fabrification of electroreduced graphene oxide−bentonite sodium composite modified electrode and its sensing application for linezolid. *Electrochim. Acta* **2014**, *133*, 49−56.
(17) Li, X. Y.; Liu, B.; Ye, W. J.; Wang, X. Y.; Sun, R. C. Effect of rectorite on the synthesis of Ag NP and its catalytic activity. *Mater. Chem. Phys.* **2015**, *151*, 301−307.
(18) Han, G. C.; Han, Y.; Wang, X. Y.; Liu, S. J.; Sun, R. C. Synthesis of organic rectorite with novel Gemini surfactants for copper removal. *Appl. Surf. Sci.* **2014**, *317*, 35−42.
(19) Wang, X. Y.; Du, Y. M.; Luo, J. W.; Lin, B. F.; Kennedy, J. F. Chitosan/organic rectorite nanocomposite films: Structure, characteristic and drug delivery behaviour. *Carbohydr. Polym.* **2007**, *69* (1), 41−49.

DOI: 10.1021/acssuschemeng.5b00404
ACS Sustainable Chem. Eng. 2015, 3, 1846−1852

(20) Liu, Y.; Deng, H. B.; Xiao, C. L.; Xie, C. F.; Zhou, X. Cytotoxicity of Calcium Rectorite Micro/Nanoparticles before and after Organic Modification. *Chem. Res. Toxicol.* **2014**, *27* (8), 1401−1410.
(21) Hummers, W. S.; Offeman, R. E. Preparation of graphitic oxide. *J. Am. Chem. Soc.* **1958**, *80* (6), 1339.
(22) Fernandez-Merino, M. J.; Guardia, L.; Paredes, J. I.; Villar-Rodil, S.; Solis-Fernandez, P.; Martinez-Alonso, A.; Tascon, J. M. D. Vitamin C Is an Ideal Substitute for Hydrazine in the Reduction of Graphene Oxide Suspensions. *J. Phys. Chem. C* **2010**, *114* (14), 6426−6432.
(23) Nethravathi, C.; Rajamathi, J. T.; Ravishankar, N.; Shivakumara, C.; Rajamathi, M. Graphite oxide-intercalated anionic clay and its decomposition to graphene-inorganic material nanocomposites. *Langmuir* **2008**, *24* (15), 8240−8244.
(24) Li, H. J.; Zhu, G.; Liu, Z. H.; Yang, Z. P.; Wang, Z. L. Fabrication of a hybrid graphene/layered double hydroxide material. *Carbon* **2010**, *48* (15), 4391−4396.
(25) Sadasivuni, K. K.; Saiter, A.; Gautier, N.; Thomas, S.; Grohens, Y. Effect of molecular interactions on the performance of poly-(isobutylene-co-isoprene)/graphene and clay nanocomposites. *Colloid Polym. Sci.* **2013**, *291* (7), 1729−1740.
(26) Stankovich, S.; Dikin, D. A.; Piner, R. D.; Kohlhaas, K. A.; Kleinhammes, A.; Jia, Y. Y.; Wang, Y.; Nguyen; SonBinh, T.; Ruoff; Rodney, S. Synthesis of graphene-based nanosheets via chemical reduction of exfoliated graphite oxide. *Carbon* **2007**, *45* (7), 1558−1565.
(27) Liu, J.; Guo, S. J.; Han, L.; Ren, W.; Liu, Y. Q.; Wang, E. Multiple pH-responsive graphene composites by non-covalent modification with chitosan. *Talanta* **2012**, *101*, 151−156.
(28) Li, X. Y.; Han, Y.; Zhong, H. Q.; Ye, W. J.; Liu, B.; Wang, X. Y.; Sun, R. C. Preparation, Characterization and Antibacterial Activity of Quaternized Carboxymethyl Chitosan/Organic Rectorite Nanocomposites. *Curr. Nanosci.* **2013**, *9* (2), 278−282.
(29) Achari, A.; Datta, K. K.; De, M.; Dravid, V. P.; Eswaramoorthy, M. Amphiphilic aminoclay-RGO hybrids: a simple strategy to disperse a high concentration of RGO in water. *Nanoscale* **2013**, *5* (12), 5316−5320.
(30) Senthilnathan, J.; Sanjeeva, RaoK.; Lin, W. H.; Liao, J. D.; Yoshimura, M. Low energy synthesis of nitrogen functionalized graphene/nanoclay hybrid via submerged liquid plasma approach. *Carbon* **2014**, *78*, 446−454.
(31) Cai, D. Y.; Song, M. Preparation of fully exfoliated graphite oxide nanoplatelets in organic solvents. *J. Mater. Chem.* **2007**, *17* (35), 3678−3680.
(32) Ling, Y. Z.; Li, X. Y.; Zhou, S. W.; Wang, X. Y.; Sun, R. C. Multifunctional cellulosic paper based on quaternized chitosan and gold nanoparticle-reduced graphene oxide via electrostatic self-assembly. *J. Mater. Chem. A* **2015**, *3* (14), 7422−7428.
(33) Kang, X. H.; Mai, Z. B.; Zou, X. Y.; Cai, P. X.; Mo, J. Y. Electrochemical biosensor based on multi-walled carbon nanotubes and Au nanoparticles synthesized in chitosan. *J. Nanosci. Nanotechnol.* **2007**, *7* (4−5), 1618−1624.
(34) Thanou, M.; Florea, B. I.; Geldof, M.; Junginger, H. E.; Borchard, G. Quaternized chitosan oligomers as novel gene delivery vectors in epithelial cell lines. *Biomaterials* **2002**, *23* (1), 153−159.
(35) Zheng, F.; Shi, X. W.; Yang, G. F.; Gong, L. L.; Yuan, H. Y.; Cui, Y. J.; Wang, Y.; Du, Y. M.; Li, Y. Chitosan nanoparticle as gene therapy vector via gastrointestinal mucosa administration: Results of an in vitro and in vivo study. *Life Sci.* **2007**, *80* (4), 388−396.

DOI: 10.1021/acssuschemeng.5b00404
ACS Sustainable Chem. Eng. 2015, 3, 1846−1852